TS fuzzy observer-based controller design for a class of discrete-time nonlinear systems

Zoltán Nagy, Zsófia Lendek, Lucian Buşoniu

***Abstract*—This paper presents an observer-based control design approach for a class of nonlinear discrete-time systems. The model nonlinearities are handled in two ways: 1) a Takagi-Sugeno fuzzy representation is used for nonlinearities that depend on measured states, and 2) nonlinearities that depend on unmeasured states are kept in their original form and handled using a slope-bound condition. The observer-based controller design conditions are given as linear matrix inequalities. The approach we propose significantly improves results in the literature by providing less restrictive design conditions. These improvements are illustrated in a detailed analytical and numerical comparison on a synthetic example; while a pendulum-on-a-cart example shows that the approach works both in simulation and in real-time experiments.**

I. Introduction

Controller and observer design are usually based on the model of the system, which in most cases is nonlinear. Linear approximations are often used, but they are valid only around the considered operating point [1]. On the other hand, many nonlinear representations are available in the literature, for example the Takagi-Sugeno (TS) fuzzy models.

The TS fuzzy representation defines the model as a convex combination of local linear models, and depending on how it is obtained it can exactly represent a nonlinear model in a compact set of the state-space [2]. This model can be used to design both controllers and observers that are valid globally in this compact set, see e.g. [3], [4], [5], [6], [7]. More advanced control strategies are discussed for example in [8], where a fuzzy sliding mode controller is presented, in [9] where the passivity-based control strategies are used for wind energy conversion system or in [10] where dissipativity and passivity based strategies are discussed.

A disadvantage of TS models is that the complexity increases exponentially with the number of nonlinearities in the model, which can lead to computationally intractable problems. To avoid that, some of the nonlinearities can be kept in their original form, as nonlinear consequents, and they can be handled using some other conditions. For example in [11] sector- and slope-bound conditions are used for the nonlinear consequents.

Most results on nonlinear observer and controller design have been developed in continuous-time, while the discrete-time case is not so well explored, see e.g. [12], [13]. However, in many real-life applications the controller is digital. Digital controllers do not change the signal values continuously, but with a specific sampling time, an effect that must be included in the analysis, leading to discrete-time controller design. For example, in [14] it is shown that feedback linearizability of continuous-time systems can be destroyed through the introduction of the usual sample and hold devices, and a discrete-time model is proposed to overcome this issue.

There are a few approaches available in the literature that tackle the problem of controller and observer design for discrete-time TS fuzzy systems with nonlinear consequents, see e.g. [11], [15], but the research in this area is not extensive; less restrictive design conditions can be obtained that can also handle a wider range of systems. This motivates us to focus on the discrete-time case in the current work.

Specifically, we consider the problem of observer-based controller design for a class of discrete-time TS fuzzy systems with nonlinear consequents. We use the fuzzy form to handle nonlinearities that depend on measured states, while the unmeasured-state nonlinearities are kept in the nonlinear consequents. The design conditions are given as linear matrix inequalities (LMI) and they are less restrictive than those existing in the literature. The work in [11] is considered as a starting point of this paper and we focus on improving the results obtained there. We have the following two main contributions:

- We use a slope-bound condition for the nonlinear consequents, while in the state-of-the-art both Lipschitz (included in slope-bound) and sector-bound conditions are needed.
- For nonlinear consequents that fulfill both Lipschitz and sector-bound conditions, our design conditions can handle a wider range of systems than what can be handled with the state-of-the-art.

There are other approaches available in the literature that consider similar problems. For example, [16] gives an approach that handles directly the nonlinearities, without the TS fuzzy form, where a slope-bound condition was used for observer design. The results in [16] were further extended in [17], [18], [19], [20], [21] to obtain less conservative design conditions. Comparing our approach to these, we have the advantage that we can handle some of the nonlinearities in the fuzzy form. This helps to obtain less restrictive design conditions and also allows to handle a wider range of nonlinear systems.

Usually, Lipschitz or slope-bound conditions are used for observer design, see e.g. [22], [11], and sector-bound conditions for controller design, see e.g. [23], [11], [24], [25], [3], [26]. One limitation of these approaches appears for observer-based controller design, since in that case the nonlinearities must fulfill both observer and controller design conditions.

*This work was supported by a grant of the Romanian National Authority for Scientific Research and Innovation, CNCS – UEFISCDI, project number PN-III-P1-1.1-TE-2016-1265, contract number 11/2018. We are grateful to Levente Nagy for his help on the practical application.

Z. Nagy, Zs. Lendek and L. Buşoniu are with the Department of Automation, Technical University of Cluj-Napoca, Romania. E-mail: {zoltan.nagy, zsofia.lendek, lucian.busoniu}@aut.utcluj.ro.

In our case, due to the form of the controller the required conditions are reduced to slope-bound conditions, and the nonlinearities do not need to fulfill the sector-bound condition. For instance, with only the slope-bound condition it is possible to include affine terms in the nonlinear consequents or nonlinear functions that are not zero at the stabilization point. This is not possible with the sector-bound condition.

The rest of the paper is organized as follows. In Section II we present the general concepts as well as some lemmas and properties that are used throughout the paper. Section III presents first the observer and then the controller design, followed by the observer-based controller design. Section IV highlights the advantages compared to the available literature. Finally, in Section V we present a comparison with the state-of-the-art for a pendulum on a cart, both in simulation and in experiments. Section VI concludes the paper and give some further research directions.

II. Preliminaries and Problem statement

Notations. Let $F = F^T \in R^{n\times n}$ be a real symmetric matrix; $F > 0$ and $F < 0$ mean that F is positive definite and negative definite, respectively. I denotes the identity matrix and 0 the zero matrix of appropriate dimensions. The symbol $*$ in a matrix indicates a transposed quantity in the symmetric position, for instance $\begin{pmatrix} P & * \\ A & P \end{pmatrix} = \begin{pmatrix} P & A^T \\ A & P \end{pmatrix}$, $A + * = A + A^T$, or $*PA = A^TPA$. The notation $\mathrm{diag}(f_1, ..., f_n)$, where $f_1, ..., f_n \in \mathbb{R}$, stands for the diagonal matrix, whose diagonal components are $f_1, ..., f_n$. Notation $\|s\|$ is the Euclidean norm of $s \in \mathbb{R}^n$. To avoid forward referencing, the rest of the notations are defined at their first use.

The classic discrete-time TS fuzzy model is a convex combination of linear models, having the form:

$$\begin{aligned} x(k+1) =& \sum_{i=1}^{s} h_i(z(k))(A_i x(k) + B_i u(k)) \\ y(k) =& \sum_{i=1}^{s} h_i(z(k)) C_i x(k), \end{aligned} \tag{1}$$

where $x(k) \in \mathbb{R}^{n_x}$ is the state vector, $u(k) \in \mathbb{R}^{n_u}$ is the control input, $y(k) \in \mathbb{R}^{n_y}$ is the measured output vector, s is the number of rules, $z(k) \in \mathbb{R}^{n_z}$ is the premise vector, and h_i, $i = 1, ..., s$ are nonlinear functions with the property

$$h_i \in [0,\, 1],\, i = 1, ..., s, \quad \sum_{i=1}^{s} h_i(z) = 1. \tag{2}$$

These nonlinear functions are called the membership functions. Matrices A_i, B_i, and C_i represent the i-th local model. Throughout this paper, the following shorthand notations are used to represent convex sums of matrix expressions:

$$F_z = \sum_{i=1}^{s} h_i(z(k)) F_i, \quad F_{z+} = \sum_{i=1}^{s} h_i(z(k+1)) F_i. \tag{3}$$

Based on this notation, (1) can be rewritten as

$$\begin{aligned} x(k+1) =& A_z x(k) + B_z u(k) \\ y(k) =& C_z x(k). \end{aligned} \tag{4}$$

A. Properties and lemmas

In order to develop our results we will use the following properties and lemmas.

Property 1 ([27]): Let A and B be matrices of appropriate dimensions and ranks, with $B = B^T > 0$. Then

$$-A^T B^{-1} A \le -A - A^T + B$$

Property 2 ([27]): (Schur complement). Let $\mathcal{M} = \mathcal{M}^T = \begin{bmatrix} M_{11} & M_{12} \\ M_{12}^T & M_{22} \end{bmatrix}$, with M_{11} and M_{22} square matrices of appropriate dimensions. Then:

$$\begin{aligned} \mathcal{M} < 0 \Leftrightarrow & \begin{cases} M_{11} < 0 \\ M_{22} - M_{12}^T M_{11}^{-1} M_{12} < 0 \end{cases} \\ \Leftrightarrow & \begin{cases} M_{22} < 0 \\ M_{11} - M_{12} M_{22}^{-1} M_{12}^T < 0 \end{cases} \end{aligned} \tag{5}$$

Lemma 1 ([27]): (Congruence) Given matrix $P = P^T$ and a full column rank matrix Q, it holds that

$$P > 0 \quad \Rightarrow \quad QPQ^T > 0.$$

Estimation and control problems are often defined as double-sum negativity problems having the form

$$F_{zz} = \sum_{i=1}^{s} \sum_{j=1}^{s} h_i(z) h_j(z) F_{ij} < 0, \tag{6}$$

with symmetric matrices F_{ij} and nonlinear functions h_i satisfying the convex sum property in (2).

Lemma 2 ([28]): Equation (6) is satisfied if the following conditions hold

$$\begin{aligned} F_{ii} <& 0 \\ \frac{2}{s-1} F_{ii} + F_{ij} + F_{ji} <& 0 \quad \forall i, j = 1, ..., s,\, i \neq j. \end{aligned} \tag{7}$$

In some cases the conditions defined are as a triple sum negativity problem having the form:

$$F_{zzz} = \sum_{i=1}^{s} \sum_{j=1}^{s} \sum_{l=1}^{s} h_i(z) h_j(z) h_l(z) F_{ijl} < 0. \tag{8}$$

Applying Lemma 2 of two of the terms in (8), the following condition is obtained:

Lemma 3: Equation (8) is satisfied if the following conditions hold

$$\begin{aligned} F_{iil} <& 0 \\ \frac{2}{s-1} F_{iil} + F_{ijl} + F_{jil} <& 0 \quad \forall i, j, l = 1, ..., s,\, i \neq j. \end{aligned} \tag{9}$$

B. Problem statement

In order to develop our results we consider the following model structure:

$$\begin{aligned} x(k+1) =& A_z x(k) + B_z u(k) + B_z G_z \psi(H_z x(k)) \\ y(k) =& C_z x(k), \end{aligned} \tag{10}$$

where $x(k)$, $u(k)$, $y(k)$ have the same meaning as in (1) and A_z, B_z, G_z, C_z are convex combinations of matrices as in (3).

We assume that the scheduling vector z only depends on measured variables. The nonlinearities that contain unmeasured states are collected in the vector function $\psi(H_z x(k))$.

A somewhat restrictive assumption we make is on the form of the unmeasured nonlinear part, i.e. $B_z G_z \psi(H_z x(k))$. Note however that such a form often appears, e.g. for mechanical systems in a classical state-space form obtained from Euler-Lagrange equations. To see this, let us consider the model of a robot arm

$$M(\theta)\ddot{\theta} = -F(\theta, \dot{\theta}) - G(\theta) + \tau, \tag{11}$$

where τ represents the torque; θ, $\dot{\theta}$ and $\ddot{\theta}$ are the angles, angular velocities and angular accelerations. $M(\theta)$ is the mass matrix, $F(\theta, \dot{\theta})$ contains the centrifugal and Coriolis forces and $G(\theta)$ contains the terms due to gravity. To obtain a classical state-space representation, the whole equation must be multiplied with the inverse of the mass matrix, leading to

$$\ddot{\theta} = -M(\theta)^{-1}F(\theta, \dot{\theta}) - M(\theta)^{-1}G(\theta) + M(\theta)^{-1}\tau. \tag{12}$$

In this context $B_z = \begin{bmatrix} 0 \\ M(\theta)^{-1} \end{bmatrix}$, with states $x = \begin{bmatrix} \theta \\ \dot{\theta} \end{bmatrix}$.

The quantity $\psi(H_z x(k)) \in \mathbb{R}^r$ is an r-dimensional vector:

$$\psi(H_z x(k)) = \begin{bmatrix} \psi_1(H_{z1}x(k)) \\ \psi_2(H_{z2}x(k)) \\ \cdots \\ \psi_r(H_{zr}x(k)) \end{bmatrix}. \tag{13}$$

One might expect that each individual ψ_l, $l = 1, ..., r$ is a function of the full vector $H_z x(k)$. However, our assumptions impose additional structure, in which ψ_l depends only on the scalar $H_{zl}x(k)$, where H_{zl} is row l in the matrix H_z. The fuzzy matrix has the form: $H_z = \sum_{i=1}^{s} h_i(z(k))H_i$, and $H_i \in \mathbb{R}^{r \times n_x}$ for $i = 1, ..., s$. A similar form of the nonlinearity – although with a constant H matrix – have been used in [17], [19].

To give an example, consider the state vector $x(k) = \begin{bmatrix} x_1(k) & x_2(k) & x_3(k) \end{bmatrix}^T$ and the nonlinearities

$$\psi = \begin{bmatrix} \psi_1(x(k)) \\ \psi_2(x(k)) \end{bmatrix} = \begin{bmatrix} \sin(x_1(k)x_2(k)) \\ \cos(x_2(k)) \end{bmatrix},$$

where $x_1 \in [-1,\ 1]$ is measured and x_2 is not measured. Since $x_1 \in [-1,\ 1]$ we can rewrite $\psi_1(x(k))$ in the form:

$$\begin{aligned} \psi_1(x(k)) =& \sin(x_1(k)x_2(k)) = \\ & \sin\Big(-\frac{1 - x_1(k)}{2}x_2(k) + \frac{1 + x_1(k)}{2}x_2(k) \Big). \end{aligned} \tag{14}$$

The membership functions are:

$$h_1(x_1(k)) = \frac{1 - x_1(k)}{2}, \quad h_2 = 1 - h_1, \tag{15}$$

and using the minimum and maximum values of x_1 leads to the following:

$$H_{11} = \begin{bmatrix} 0 & -1 & 0 \end{bmatrix}, \quad H_{12} = \begin{bmatrix} 0 & 1 & 0 \end{bmatrix}.$$

For $\psi_2(x(k))$ we have $H_{21} = H_{22} = \begin{bmatrix} 0 & 1 & 0 \end{bmatrix}$, and that leads to

$$\begin{aligned} H_z =& h_1(x_1(k))H_1 + h_2(x_1(k))H_2 = \\ & h_1(x_1(k)) \begin{bmatrix} 0 & -1 & 0 \\ 0 & 1 & 0 \end{bmatrix} + h_2(x_1(k)) \begin{bmatrix} 0 & 1 & 0 \\ 0 & 1 & 0 \end{bmatrix}. \end{aligned}$$

To develop our results, the elements in vector $\psi(H_z x(k))$ must fulfill the following assumption.

Assumption 1: For any $i \in \{1, ..., r\}$ there exist constants $0 < b_i < \infty$, so that

$$0 \leq \frac{\psi_i(v) - \psi_i(w)}{v - w} \leq b_i, \quad \forall v, w \in \mathbb{R}, v \neq w. \tag{16}$$

This assumption allows us to handle nonlinearities in their original form, without converting them into TS fuzzy representation. Similar assumptions were used in [16], [17], [19], [29], but for linear dynamics. To overcome this limitation, we allow the rest of the dynamics to be nonlinear and handle them with TS fuzzy modelling.

In view of (16), there exist $\delta_i(k) \in [0,\ b_i]$, so that for any v, $w \in \mathbb{R}$

$$\psi_i(v) - \psi_i(w) = \delta_i(k)(v - w). \tag{17}$$

We use the notation $\delta(k)$, to handle all δ_i in one matrix: $\delta(k) = \mathrm{diag}(\delta_1(k), ..., \delta_r(k))$.

III. Main results

In this section, sufficient conditions will be developed for observer-based controller design. We consider the following observer structure:

$$\begin{aligned} \hat{x}(k+1) =& A_z\hat{x}(k) + B_z G_z \psi\left(H_z\hat{x}(k) + L_\psi(y(k) - \hat{y}(k))\right) \\ & + B_z u(k) + L_z(y(k) - \hat{y}(k)) \\ \hat{y}(k) =& C_z\hat{x}(k), \end{aligned} \tag{18}$$

where $L_z = \sum_{i=1}^{s} h(z(k))L_i$ and $L_\psi = \sum_{i=1}^{s} h(z(k))L_{\psi i}$, contain the observer gains. The term L_ψ adds an extra degree of freedom, to obtain less conservative conditions.

The controller has the form:

$$u(k) = -K_z Q_z^{-1}\hat{x}(k) - G_z\psi(H_z\hat{x}(k) + L_\psi(y(k) - \hat{y}(k))), \tag{19}$$

where $K_z = \sum_{i=1}^{s} h(z(k))K_i$ contains the controller gains, and with $Q_z^{-1} = \left(\sum_{i=1}^{s} h(z(k))Q_i\right)^{-1}$ an extra degree of freedom is added. The term $G_z\psi(H_z\hat{x}(k) + L_\psi(y(k) - \hat{y}(k)))$ is used to compensate the unmeasured-state dependent nonlinearities in the closed loop dynamics.

Based on (10) and (18) and defining the estimation error as $e(k) = x(k) - \hat{x}(k)$, the error dynamics are

$$\begin{aligned} & e(k+1) = (A_z - L_z C_z)e(k) \\ & + B_z G_z \left(\psi(H_z x(k)) - \psi(H_z\hat{x}(k) + L_\psi(y(k) - \hat{y}(k)))\right). \end{aligned} \tag{20}$$

This can be further transformed by considering (17):

$$\begin{aligned} e(k+1) =& (A_z - L_z C_z)e(k) \\ & + B_z G_z \delta(k) \left(H_z x(k) - H_z\hat{x}(k) - L_\psi(y(k) - \hat{y}(k))\right) \\ =& (A_z - L_z C_z)e(k) \\ & + B_z G_z \delta(k) \left(H_z e(k) - L_\psi C_z e(k)\right). \end{aligned} \tag{21}$$

By denoting $\eta(k) := (H_z - L_\psi C_z)e(k)$, we obtain:

$$e(k+1) = (A_z - L_z C_z)e(k) + B_z G_z \delta(k)\eta(k). \tag{22}$$

Next, considering the control law (19) in (10) the following closed loop system is obtained:

$$\begin{aligned} x(k+1) =& (A_z - B_z K_z Q_z^{-1})x(k) + B_z K_z Q_z^{-1} e(k) \\ &+ B_z G_z \delta(k)\eta(k) \\ \eta(k) =& (H_z - L_\psi C_z)e(k). \end{aligned} \tag{23}$$

The obtained form in (23) depends on $\delta(k)\eta(k)$. To develop the design conditions, we consider the estimated states, $\hat{x}(k)$, in closed loop instead of $x(k)$:

$$\hat{x}(k+1) = (A_z - B_z K_z Q_z^{-1})\hat{x}(k) + L_z C_z e(k), \tag{24}$$

which has a less complex expression, and we obtain the following augmented dynamics:

$$\begin{aligned} \begin{bmatrix} \hat{x}(k+1) \\ e(k+1) \end{bmatrix} =& \begin{bmatrix} A_z - B_z K_z Q_z^{-1} & L_z C_z \\ 0 & A_z - L_z C_z \end{bmatrix} \begin{bmatrix} \hat{x}(k) \\ e(k) \end{bmatrix} \\ &+ \begin{bmatrix} 0 \\ B_z G_z \end{bmatrix} \delta(k)\eta(k) \\ \eta(k) =& (H_z - L_\psi C_z)e(k). \end{aligned} \tag{25}$$

If both the error dynamics, $e(k)$, and the estimated states, $\hat{x}(k)$, are stable at the origin, then so are the system states, $x(k)$. For this reason in the following analysis we will consider (25).

Next we define the conditions for observer design (Section III-A) and for controller design (Section III-B) respectively, followed by the main result, which proves that the independent designs indeed lead to a stable closed-loop system (Section III-C).

A. Observer design

In this section we consider the estimation error in (22) repeated here for convenience:

$$e(k+1) = (A_z - L_z C_z)e(k) + B_z G_z \delta(k)\eta(k),$$

and develop sufficient conditions to prove exponential stability of these error dynamics.

Theorem 1: Consider system (10) and observer (18). If there exist matrices $M = M^T = \text{diag}(m_1, ..., m_r) > 0$, S, $P_i = P_i^T > 0$, N_i, $W_{\psi i}$, $i = 1, ..., s$, and constant $\epsilon > 0$ so that

$$\begin{aligned} F_{iil} \leq& 0 \\ \frac{2}{s-1} F_{iil} + F_{ijl} + F_{jil} \leq& 0 \quad \forall i, j, l = 1, ..., s,\ i \neq j. \end{aligned} \tag{26}$$

where

$$F_{ijl} = \begin{bmatrix} -P_i + \epsilon I & * & * \\ MH_i + W_{\psi i} C_j & \nu(M) & * \\ SA_i - N_i C_j & SB_i G_j & P_l - S - S^T \end{bmatrix}, \tag{27}$$

and

$$\nu(M) = -2M\text{diag}(\frac{1}{b_1}, ..., \frac{1}{b_r}), \tag{28}$$

then the observer states defined in (18) converge exponentially to the real system states in (10). The observer gains can be recovered from $L_i = S^{-1} N_i$, $L_{\psi i} = M^{-1} W_{\psi i}$.

Proof: Consider the Lyapunov function candidate $V = e(k)^T P_z e(k)$, where $P_z = P_z^T = \sum_{i=1}^{s} h_i(z(k)) P_i > 0$, and the difference

$$\Delta V = e(k+1)^T P_{z+} e(k+1) - e(k)^T P_z e(k). \tag{29}$$

We denote $\zeta(k) = \begin{bmatrix} e(k)^T & (\delta(k)\eta(k))^T \end{bmatrix}^T$, which leads to

$$\Delta V = \zeta(k)^T \Sigma\, \zeta(k), \tag{30}$$

where

$$\begin{aligned} \Sigma =& \begin{bmatrix} \mathcal{E} & * \\ G_z^T B_z^T P_{z+}(A_z - L_z C_z) & *P_{z+} B_z G_z \end{bmatrix} \\ \mathcal{E} =& (A_z - L_z C_z)^T P_{z+}(A_z - L_z C_z) - P_z. \end{aligned} \tag{31}$$

If $\Delta V < 0$ then the error dynamics are stable. Since $P_{z+} = P_{z+}^T > 0$, then the positive or negative definiteness of the term at (2,2) in Σ depends only on $B_z G_z$. This condition is very conservative. To overcome this issue we add some additional terms. Next, consider the inequality:

$$\zeta(k)^T \Sigma\, \zeta(k) + \zeta(k)^T \Gamma\, \zeta(k) \leq 0, \tag{32}$$

where

$$\Gamma = \begin{bmatrix} \epsilon I & * \\ \mathcal{B} & \nu(M) \end{bmatrix}, \quad \mathcal{B} = MH_z + ML_\psi C_z, \tag{33}$$

and $\nu(M)$ is defined in (28). Let us now examine $\zeta(k)^T \Gamma \zeta(k)$:

$$\begin{aligned} \zeta(k)^T \Gamma\, \zeta(k) =& \epsilon \|e(k)\|^2 + * \nu(M)\delta(k)\eta(k) \\ &+ 2e(k)^T (H_z^T + C_z^T L_\psi^T) M \delta(k)\eta(k) \end{aligned} \tag{34}$$

We know that $\eta(k) = (H_z + L_\psi C_z)e(k)$, which leads to:

$$-\zeta(k)^T \Gamma\, \zeta(k) = -\epsilon \|e(k)\|^2 - 2\eta(k)^T \mathcal{D} \eta(k), \tag{35}$$

where $\mathcal{D} = M\delta(k) + 2\delta(k)^T \nu(M)\delta(k)$. Since all the elements in $\mathcal{D}$ are on the main diagonal we can examine the elements:

$$m_i \delta_i(k) \left(1 - \tfrac{1}{b_i}\delta_i(k)\right). \tag{36}$$

Based on (17) $\delta_i(k) \leq b_i$, from where we can conclude that $\mathcal{D} \geq 0$, and this leads to:

$$-\zeta(k)^T \Gamma\, \zeta(k) \leq -\epsilon \|e(k)\|^2 \leq 0. \tag{37}$$

Therefore, if $\zeta(k)^T \Sigma\, \zeta(k) + \zeta(k)^T \Gamma\, \zeta(k) \leq 0$, then $\Delta V < 0$.

To obtain LMI conditions, consider the matrix inequality $\Sigma + \Gamma \leq 0$. Then,

$$\begin{bmatrix} \mathcal{E} + \epsilon I & * \\ G_z^T B_z^T P_{z+}(A_z - L_z C_z) + \mathcal{B} & *P_{z+} B_z G_z + \nu(M) \end{bmatrix} \leq 0. \tag{38}$$

Due to the coupled terms in $\mathcal{E}$, the inequality is bilinear. Applying a Schur complement in the form:

$$\begin{bmatrix} -P_z + \epsilon I & * \\ \mathcal{B} & \nu(M) \end{bmatrix} + \begin{bmatrix} \mathcal{F}^T \\ G_z^T B_z^T \end{bmatrix} P_{z+} \begin{bmatrix} \mathcal{F} & B_z G_z \end{bmatrix} \leq 0 \tag{39}$$

with $\mathcal{F} = A_z - L_z C_z$, leads to:

$$\begin{bmatrix} -P_z + \epsilon I & * & * \\ \mathcal{B} & \nu(M) & * \\ \mathcal{F} & B_z G_z & -P_{z+}^{-1} \end{bmatrix} \leq 0. \tag{40}$$

Next we consider full rank matrix $S \in \mathbb{R}^{n_x \times n_x}$. Congruence with $\mathrm{diag}[I\ I\ S]$ leads to the following:

$$\begin{bmatrix} -P_z + \epsilon I & * & * \\ \mathcal{B} & \nu(M) & * \\ S\mathcal{F} & SB_zG_z & -SP_{z+}^{-1}S^T \end{bmatrix} \leq 0. \quad (41)$$

Using Property 1 we have $-SP^{-1}S^T \leq P - S - S^T$ and we obtain:

$$\begin{bmatrix} -P_z + \epsilon I & * & * \\ MH_z + ML_\psi C_z & \nu(M) & * \\ SA_z - SL_zC_z & SB_zG_z & P_{z+} - S - S^T \end{bmatrix} \leq 0. \quad (42)$$

By denoting $N_z := SL_z$ and $W_\psi := ML_\psi$, and applying Lemma 3, the LMI conditions in Theorem 1 are obtained. ■

Note that, by using a fuzzy Lyapunov function the conservatism is already reduced with respect to a common quadratic one. Naturally the approach is still conservative, and this conservatism can be further reduced by using more sums in the Lyapunov functions, using delayed Lyapunov functions, developing asymptotically necessary and sufficient conditions etc. However, such generalizations are left for future research.

B. Controller design

This part presents our conditions for controller design assuming that all states are available.

Lemma 4: Consider system (10) with the assumption that all the states are available, and consider the following control law:

$$u(k) = -K_zQ_z^{-1}x(k) - G_z\psi(Hx(k)). \quad (43)$$

If there exist matrices $P_z = P_z^T > 0$, and controller gain matrices K_i, Q_i, where $i = 1, ..., s$, such that,

$$\begin{aligned} F_{iil} &< 0 \\ \frac{2}{s-1}F_{iil} + F_{ijl} + F_{jil} &< 0 \quad \forall i, j, l = 1, ..., s,\ i \neq j, \end{aligned} \quad (44)$$

where

$$F_{ij} = \begin{bmatrix} -Q_i - Q_i^T + P_i & * \\ B_jK_i + A_jQ_i & -P_l \end{bmatrix}, \quad (45)$$

then the closed loop system is asymptotically stable at the origin.

Proof: Based on (10) and (43) the closed loop system is:

$$x(k+1) = (A_z - B_zK_zQ_z^{-1})x(k). \quad (46)$$

Consider the Lyapunov function candidate $V(x(k)) = x(k)^TP_z^{-1}x(k)$, and the difference

$$\Delta V = x(k+1)^TP_{z+}^{-1}x(k+1) - x(k)^TP_z^{-1}x(k) \quad (47)$$

This can be written as:

$$\Delta V = x(k)^T\left(\mathcal{H}^TP_{z+}^{-1}\mathcal{H} - P_z^{-1}\right)x(k) \quad (48)$$

with $\mathcal{H} := A_z - B_zK_zQ_z^{-1}$. We have:

$$\left(\mathcal{H}^TP_{z+}^{-1}\mathcal{H} - P_z^{-1}\right) < 0. \quad (49)$$

Applying the Schur complement we have

$$\begin{bmatrix} -P_z^{-1} & * \\ A_z - B_zK_zQ_z^{-1} & -P_{z+} \end{bmatrix} < 0. \quad (50)$$

Congruence with $\begin{bmatrix} Q_z^T & 0 \\ 0 & I \end{bmatrix}$ leads to

$$\begin{bmatrix} -Q_z^TP_z^{-1}Q_z & * \\ A_zQ_z - B_zK_z & -P_{z+} \end{bmatrix} < 0. \quad (51)$$

Using Property 1 on $-Q_z^TP_z^{-1}Q_z$ leads to

$$\begin{bmatrix} -Q_z^T - Q_z + P_z & * \\ A_zQ_z - B_zK_z & -P_{z+} \end{bmatrix} \quad (52)$$

Finally, the sufficient LMI conditions (44) are obtained by applying Lemma 2. ■

C. Observer-based control

In closing of our analytical development, we prove that stability is ensured by using in tandem the controller and observer obtained by using Theorem 1 and Lemma 4 for system (10).

Theorem 2: Consider system (10). If there exist controller gains Q_i, K_i, where $i = 1, ..., s$, which fulfill (44) and if there exist observer gains $L_{\psi i}$, L_i, where $i = 1, ..., s$ which fulfill (26), then the augmented system states in (25) are asymptotically stable at the origin.

Proof: Consider the Lyapunov function $V_c(\hat{x}(k)) = \hat{x}(k)^TP_c\hat{x}(k)$ with $P_c = P_c^T = \sum_{i=1}^s h_i(z(k))P_{ci} > 0$, and $P_{c^+} = \sum_{i=1}^s h_i(z(k+1))P_{ci}$, so that:

$$\mathcal{H}^TP_{c^+}\mathcal{H} - P_c < 0, \quad \mathcal{H} := A_z - B_zK_zQ_z^{-1}, \quad (53)$$

i.e. it ensures stability for (46). On the other hand, consider the Lyapunov function $V_o(e(k)) = e(k)^TP_oe(k)$ with $P_o = P_o^T = \sum_{i=1}^s h_i(z(k))P_{oi} > 0$, and $P_{o^+} = \sum_{i=1}^s h_i(z(k+1))P_{oi}$, so that:

$$\Delta V = \zeta(k)^T \begin{bmatrix} \mathcal{E} & * \\ G_z^TB_z^TP_{o^+}(A_z - L_zC_z) & *P_{o^+}B_zG_z \end{bmatrix} \zeta(k) < 0, \quad (54)$$

i.e. it ensures the stability of (20), with the notations $\mathcal{E} := (A_z - L_zC_z)^TP_{o^+}(A_z - L_zC_z) - P_o$, and $\zeta(k) = \begin{bmatrix} e(k)^T & (\delta(k)\eta(k))^T \end{bmatrix}^T$. Since $\eta(k) = (H - L_\psi C_z)e(k)$, (54) can be rewritten as:

$$\begin{aligned} &e(k)^T(\mathcal{G}^TP_{o^+}\mathcal{G} - P_o)e(k) < 0 \\ &\mathcal{G} := A_z - L_zC_z + B_zG_z\delta(k)(H - L_\psi C_z). \end{aligned} \quad (55)$$

Next, consider (25), rewritten as

$$\begin{bmatrix} \hat{x}(k+1) \\ e(k+1) \end{bmatrix} = \begin{bmatrix} \mathcal{H} & \mathcal{J} \\ 0 & \mathcal{G} \end{bmatrix} \begin{bmatrix} \hat{x}(k) \\ e(k) \end{bmatrix}, \quad (56)$$

where $\mathcal{J} := L_zC_z$, and the candidate Lyapunov function:

$$V(\hat{x}(k), e(k)) = \begin{bmatrix} \hat{x}(k) \\ e(k) \end{bmatrix}^T \begin{bmatrix} \alpha P_c & 0 \\ 0 & P_o \end{bmatrix} \begin{bmatrix} \hat{x}(k) \\ e(k) \end{bmatrix}. \quad (57)$$

$\Delta V < 0$ if

$$\begin{bmatrix} \mathcal{H}^T & 0 \\ \mathcal{J}^T & \mathcal{G}^T \end{bmatrix} \begin{bmatrix} \alpha P_{c^+} & 0 \\ 0 & P_{o^+} \end{bmatrix} \begin{bmatrix} \mathcal{H} & \mathcal{J} \\ 0 & \mathcal{G} \end{bmatrix} - \begin{bmatrix} \alpha P_c & 0 \\ 0 & P_o \end{bmatrix} < 0 \quad (58)$$

i.e.

$$\begin{bmatrix} \alpha(\mathcal{H}^TP_{c^+}\mathcal{H} - P_c) & \alpha\mathcal{H}^TP_{c^+}\mathcal{J} \\ * & \alpha\mathcal{J}^TP_{c^+}\mathcal{J} + \mathcal{G}^TP_{o^+}\mathcal{G} - P_o \end{bmatrix} < 0. \quad (59)$$

Since $\mathcal{H}P_{c^+}\mathcal{H} - P_c < 0$, it is invertible, and a Schur complement leads to

$$\begin{aligned}&\mathcal{G}^T P_{o^+}\mathcal{G} - P_o + \alpha\mathcal{J}^T P_{c^+}\mathcal{J} \\ &- \alpha\mathcal{J}^T P_{c^+}\mathcal{H}(\mathcal{H}^T P_{c^+}\mathcal{H} - P_c)^{-1}\mathcal{H}^T P_{c^+}\mathcal{J} < 0.\end{aligned} \tag{60}$$

Since $\mathcal{G}^T P_{o^+}\mathcal{G} - P_o < 0$, and both other terms are multiplied with α, then there exists a constant $\alpha > 0$ that (60) is true. So, it is proved that if an observer and controller can be designed based on Theorem 1 and Lemma 4, then also an observer-based controller can be obtained by the combination of the two. ■

IV. Analytical and numerical comparison with existing results

In this section we highlight the advantages of our approach compared to state-of-the-art conditions. Most existing results using TS fuzzy models with nonlinear consequents are in continuous-time, and only a few handle the discrete-time case [12], [11].

As to controller design, recently [26] defined a cone-bound sector condition for the nonlinear consequents. This condition is not necessary in our approach. Since we focus on observer-based controller design, we compare our approach to [11], the closest reference to our work.

A. Comparison of the conditions for nonlinear consequents

As a first basis for comparison, we consider the nonlinear terms $\psi(\cdot)$. In our approach the nonlinear terms need to fulfill Assumption 1, which is a slope-bound condition, while in [11] these nonlinearities need to fulfill two conditions: a sector-bound condition and a Lipschitz condition. The sector-bound condition is defined as

$$\psi_i(x(k)) \in \text{co}\{0, E_i x(k)\}, \tag{61}$$

where E_i is a vector that defines a linear combination of the states, and $\text{co}\{x, y\}$ is the convex hull of x, y. Some types of nonlinearities satisfy the slope-bound conditions, while others are sector-bounded. Of course, there are nonlinearities that fulfill both, but to highlight the difference, here are some examples which are slope-bounded, but not sector-bounded:

$$\begin{aligned}\psi_1(x) =& x^2 + 2x + 3, \quad x \in [-1, 1] \\ \psi_2(x) =& e^x, \quad x \in [0, 2]\end{aligned} \tag{62}$$

With the slope-bound condition, affine terms can be included in the nonlinearities, as well as other terms that are not zero at $x = 0$; such elements can not be handled by (61). To summarize the class of nonlinearities that can be handled with our approach or with [11] see Fig. 1, where the slope-bound condition is for our approach, and the intersection of Lipschitz and sector-bound conditions (hatched surface) is for [11].

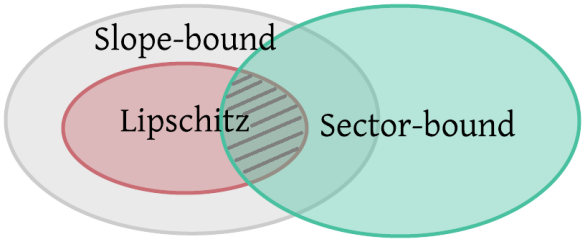

Fig. 1. Conditions on local nonlinearities

B. Comparison for observer design

To highlight the advantages of the observer design in our Theorem 1 compared to Theorem 1 in [11], we present here the LMI condition used in Theorem 1 in [11]:

$$\begin{bmatrix} -P_{oi} + R^T\Theta\overline{\Lambda}_o R & * & * \\ 0 & -\Lambda_o & * \\ S_oA_i + Y_jC_{2i} & S_oG_{xi} + Y_jG_{yi} & P_{ol} - S_o - S_o^T \end{bmatrix} < 0, \tag{63}$$

To build a correspondence between Theorem 1 in [11] and our Theorem 1, we consider (27) with $W_{\psi i} = 0$, $H_i = H$, $B_i = B$, for $i = 1, ..., s$, furthermore in (63) we take $P_{oi} := P_i$, $S_{oi} := S_i$, $Y_j := N_i$, $G_{xi} := BG_i$, $G_{yi} := 0$, $C_{2i} := C_i$ for $i = 1, ..., s$, and function $\phi() := \psi()$. In [11] the notation $\phi_e(k) = \phi(x(k)) - \phi(\hat{x}(k))$ was used. To match this with our approach we consider $\phi_e(k) := \delta(k)\eta(k)$, with $\delta_i(k) \in [0, b_i]$, for $i = 1, ..r$, and $R = H$, $\overline{\Lambda}_o := \Lambda_o = M$, $\Theta := \text{diag}(b_1^2, ..., b_r^2)$.

The Lipschitz condition used in [11] is:

$$\begin{aligned}\|\phi_i(x(k)) - \phi_i(\hat{x}(k))\| \leq \theta_i \|R_i(x(k) - \hat{x}(k))\|, \\ i = 1, ..., r\end{aligned} \tag{64}$$

It is assumed that the nonlinearities $\psi(\cdot)$ satisfy both (16) and (64). Since our conditions prove exponential stability due to the term ϵI, which is not the case in Theorem 1 of [11], we consider for the purposes of this comparison $\epsilon = 0$. We can see that the elements consists at $(3,1)$, $(3,2)$, $(3,3)$ of the matrix and their transposes are the same in (63) and (27). The elements that are different in (63) are:

$$\mathcal{A}_1 = \begin{bmatrix} R^T\Theta\Lambda_o R & * \\ 0 & -\Lambda_o \end{bmatrix}. \tag{65}$$

In what follows, we show that due to the terms in (65) our conditions are less conservative than the conditions in Theorem 1 in [11]. By pre- and post multiplying $\mathcal{A}_1$ with $\begin{bmatrix} e(k) \\ \phi_e(k) \end{bmatrix}^T$ we obtain

$$\begin{aligned}&\begin{bmatrix} e(k) \\ \phi_e(k) \end{bmatrix}^T \mathcal{A}_1 \begin{bmatrix} e(k) \\ \phi_e(k) \end{bmatrix} = \\ &e(k)^T R^T\Theta\Lambda_o Re(k) - \phi_e(k)^T\Lambda_o\phi_e(k),\end{aligned} \tag{66}$$

and because of the Lipschitz condition in (64) we have:

$$e(k)^T R^T\Theta\Lambda_o Re(k) - \phi_e(k)^T\Lambda_o\phi_e(k) \geq 0. \tag{67}$$

This condition was used to prove Theorem 1 in [11]. Now consider (65) with our notations:

$$\mathcal{A}_1 = \begin{bmatrix} H^T \text{diag}(b_1^2, ..., b_r^2) MH & * \\ 0 & -M \end{bmatrix}. \tag{68}$$

Pre- and post multiplying with $\zeta(k)^T$ and $\zeta(k)$, we obtain:

$$e(k)^T H^T \text{diag}(b_1^2, .., b_r^2) MHe(k) - \eta(k)^T \delta(k)^T M \delta(k) \eta(k) \tag{69}$$

Since $W_\psi = 0$, then $\eta(k) = He(k)$, leading to:

$$\eta(k)^T \left(\text{diag}(b_1^2, ..., b_r^2) M - \delta(k) M \delta(k) \right) \eta(k) \tag{70}$$

All matrices are diagonal, so we can examine just their diagonal elements:

$$m_i \left(b_i^2 - \delta_i(k)^2 \right), \tag{71}$$

and $m_i > 0$, so we have

$$b_i^2 - \delta_i(k)^2 \geq 0, \tag{72}$$

which is true because $b_i \geq \delta_i(k)$.

Now we consider our Assumption (1), where the diagonal elements lead to (36), repeated here for clarity:

$$m_i \left(\delta_i(k) - \frac{\delta_i(k)^2}{b_i} \right).$$

Since $m_i > 0$, we have

$$\delta_i(k) - \frac{\delta_i(k)^2}{b_i} \geq 0 \Leftrightarrow b_i \delta_i(k) - \delta_i(k)^2 \geq 0, \tag{73}$$

which is true because $b_i \geq \delta_i(k)$. This proves that our conditions are more relaxed, as we only need $b_i \delta_i(k)$ instead of b_i^2:

$$0 \leq b_i \delta_i(k) - \delta_i(k)^2 \leq b_i^2 - \delta_i(k)^2. \tag{74}$$

To further see the advantages, consider the following numerical example.

Example 1: Model (10) is considered with matrices

$$A_1 = A_2 = \begin{bmatrix} 1 & 0.008 \\ 0 & a_1 \end{bmatrix}, \; A_3 = A_4 = \begin{bmatrix} 1 & 0.008 \\ 0 & 0.99 \end{bmatrix}, \; B = \begin{bmatrix} 0 \\ 1 \end{bmatrix}$$
$$G_1 = G_3 = a_2, \; G_2 = G_4 = 0.0027, \; C = \begin{bmatrix} 1 & 0 \end{bmatrix}. \tag{75}$$

In this model we have two parameters $a_1 \in [-1, 3]$ and $a_2 \in [-1.5, 1.5]$, and we look for feasible solutions with both Theorem 1 and Theorem 1 in [11].

A single unmeasured-state-dependent nonlinearity is included in $\psi(Hx(k))$, which satisfies (16) with $b = 1$ and $H = \begin{bmatrix} 0 & 1 \end{bmatrix}$. The values for which feasible solutions have been obtained can be seen in Fig. 2. Theorem 1 provides a wider range compared to Theorem 1 of [11], and the range can be further extended by considering the injection term W_ψ.

C. Comparison for controller design

In the case when we consider only the controller design, i.e. all variables are known, one advantage stems from the matching condition $B_z G_z \psi(\cdot)$, which leads to the cancellation of the nonlinear consequents. In Corollary 1 of [11], the terms

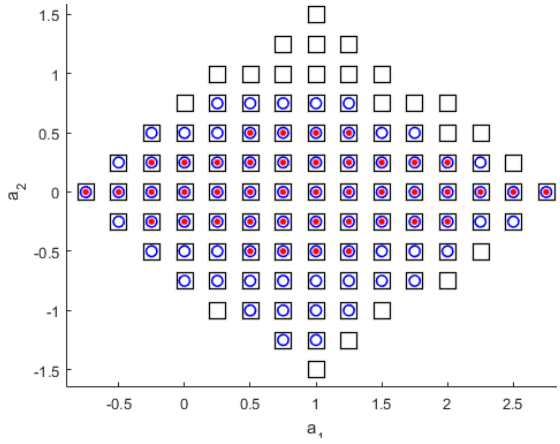

Fig. 2. $b = 1$: '.'-Theorem 1 from [11], 'o'-Theorem 1 with $W_\psi = 0$, '□'-Theorem 1

in the LMI condition (written with our notations) are defined as:

$$F_{ijl} = \begin{bmatrix} P_i - Q - Q^T & * & * \\ EQ & -2\Lambda_c & * \\ A_i Q + B_i V_{aj} & G_i \Lambda_c + B_i V_{bj} & -P_l \end{bmatrix}, \tag{76}$$

while the corresponding term in our Theorem 4 is:

$$F_{ijl} = \begin{bmatrix} P_i - Q_i - Q_i^T & * \\ B_j K_i + A_j Q_i & -P_l \end{bmatrix}. \tag{77}$$

We generalize the Q matrix by considering the fuzzy form: $Q_z = \sum_{i=1}^{s} h_i(z) Q_i$, which provides less restrictive conditions than the constant Q in Corollary 1 of [11]. When $Q_z = Q$ in (76) we have only the elements at positions (1,1), (1,3), (3,1) and (3,3) of (76), therefore (77) is necessary for (76), but not vice versa. In (76) the condition depends on E which makes it sector-bound-dependent condition, hence more restrictive.

Note that a *disadvantage* of our approach compared to [11] is that the model is restricted so that the input is matching the nonlinearity. This structure is not restricted in Corollary 1 of [11]. Next we highlight the advantages of our approach on a numerical example.

Example 2: Consider (10) with matrices:

$$A_1 = \begin{bmatrix} 1 & 0.008 \\ 0 & -1 \end{bmatrix}, \; A_2 = \begin{bmatrix} 1 & 0.008 \\ 0 & 0.9 \end{bmatrix}, \; B = \begin{bmatrix} 0 \\ 1 \end{bmatrix},$$
$$H = \begin{bmatrix} 0 & 1 \end{bmatrix}, \; G_1 = -0.027, \; G_2 = 0.027,$$

membership functions $h_1(x_1(k)) = \frac{1 - \sin(x_1)}{2}$, $h_2(x_1(k)) = 1 - h_1(x_1(k))$, and a nonlinear consequent $\psi(\cdot)$ that fulfills the sector bound condition with $E = [0, \; \alpha]$, where α is a varying parameter. Note that for the design the sector-bound is used, and the form of the nonlinearity is not important. Therefore we do not specify the nonlinearity for this example.

In order to apply Corollary 1 in [11] we use

$$\tilde{G}_1 = BG_1 = \begin{bmatrix} 0 \\ -0.027 \end{bmatrix}, \; \tilde{G}_2 = BG_2 = \begin{bmatrix} 0 \\ 0.027 \end{bmatrix}.$$

With these, we obtain feasible solutions for values $\alpha \leq 14$. Since in our case in Theorem 4 the LMI conditions do not depend on the sector-bound they are feasible for any values of α.

TABLE I
PARAMETER TABLE

Notation	Value	Description
g $[m^s/s]$	9.8	gravitational acceleration
m [kg]	0.2	mass of pendulum
M [kg]	1.61	mass of cart
γ [N/rad/s]	0.4898	friction coefficient
l [m]	0.67	length of pendulum
J $[kg\,m^2]$	0.0232	moment of inertia
K_m [-]	6.5914	PWM gain
σ [rad/s]	15	max angular velocity

D. Comparison for observer-based control

For observer-based controller design both observer and controller design conditions must be fulfilled.

Also in this context our approach provides less restrictive design conditions than the approach of [11] since for the controller design we do not require the sector-bound condition.

V. Case study: a pendulum system

In this section we test the proposed observer-based controller in experiments involving a pendulum on a cart. In the sequel we present the model of the pendulum, which is followed by a comparison with the state of the art in Section V-A. Next, the simulation results are presented in Section V-B, and finally, experimental results in Section V-C close the section.

The model for the pendulum system is adopted from [22] and in continuous time has the following form:

$$\begin{aligned}\dot{x}_1 =& x_2\\ \dot{x}_2 =& \rho_1(x_1)x_2+\rho_2(x_1)\rho_3(x_1)\psi(Hx)+\rho_2(x_1)(\tilde{u}+\beta(x_1))\\ y =& x_1\end{aligned} \tag{78}$$

where x_1 is the angle of the pendulum and x_2 is the angular velocity. The system has an unstable equilibrium point at the pointing up position and the purpose of the controller is to stabilize the system at that point by moving the cart. The nonlinear functions are:

$$\begin{aligned}\psi(Hx) =& x_2^2 + 2\sigma x_2, \quad H = \begin{bmatrix}0 & 1\end{bmatrix}\\ \rho_1(x_1) =& \frac{-\gamma + 2\sigma a m^2 l^2 \cos(x_1)\sin(x_1)}{\alpha(x_1)}\\ \rho_2(x_1) =& \frac{-K_m a m l \cos(x_1)}{\alpha(x_1)}\\ \rho_3(x_1) =& \frac{ml\sin(x_1)}{K_m}, \quad \beta(x_1) = -\frac{g\sin(x_1)}{a\cos(x_1)},\end{aligned} \tag{79}$$

where $\alpha(x_1) = (J+ml^2) - a(ml\cos(x_1))^2$, $a = 1/(M+m)$ and the rest of the parameters can be found in Table I.

The nonlinearity which depends on the unmeasured states is $\psi(Hx)$ and to fulfill Assumption 1 it is assumed that the angular velocity is bounded $x_2 \in [-\sigma, \sigma]$, which will be verified *a posteriori*. Under this condition Assumption 1 is satisfied with $b = 4\sigma$.

Since $\beta(x_1)$ depends only on the measured state, x_1, we can eliminate its effect by defining $\tilde{u} = u - \beta(x_1)$. Now (78) matches the form required for (10).

Based on considerations from the real application, the sampling time is taken $T_s = 0.01[s]$, and a discrete-time state-space model obtained by forward Euler discretization is

$$\begin{aligned}x(k+1) =& A(x_1(k))x(k) + B(x_1(k))u(k)\\ &+ B(x_1(k))G(x_1(k))\psi(Hx(k))\\ y(k) =& Cx(k),\end{aligned} \tag{80}$$

where

$$\begin{aligned}A(x_1(k)) =& \left(I + T_s\begin{bmatrix}0 & 1\\ 0 & \rho_1(x_1(k))\end{bmatrix}\right),\ C = \begin{bmatrix}1 & 0\end{bmatrix}\\ B(x_1(k)) =& Ts\begin{bmatrix}0\\ \rho_2(x_1(k))\end{bmatrix},\ G(x_1(k)) = \rho_3(x_1(k)).\end{aligned} \tag{81}$$

A. Comparison with the state of the art

The observer should converge rapidly to the system states. The convergence can be manipulated by considering a decay rate [30], which defines the following relationship: $\|e(k)\| \leq \omega^k\chi\|e(0)\|$. Thus, the error at time step k decreases exponentially compared to the initial error with a decay rate $\omega \in (0,\ 1)$, and some Lyapunov function dependent constant χ.

It can be seen that both $\rho_1(\cdot)$ and $\psi(\cdot)$ depend on the maximum angular velocity σ, a parameter that needs to be verified *a posteriori* to see if the obtained results indeed fulfill the assumption that the angular velocity is below the maximum. If this condition is not satisfied, then we have no theoretical guarantee for the observer. Thus, the greater the value of σ, the better.

For the observer design we consider the case when the rod of the pendulum can make a full circle, therefore the compact set of the state space under which the TS model is defined is $x_1 \in [-\pi,\ \pi]$ and $x_2 \in [-\sigma,\ \sigma]$. We use the sector-nonlinearity approach [2] to obtain the local models.

Using [11] for observer design with a value of the decay rate $\omega = 0.31$, the maximum angular velocity σ for which a feasible solution can be found is $\sigma = 45[rad/s]$. Using our approach with no injection term ($L_\psi = 0$) increases this to $\sigma = 65[rad/s]$, and if we use the injection term we have $\sigma = 114[rad/s]$. We can see that using our approach with no injection term leads to a 44% increase of the maximum angular velocity, while with the injection term, this value is increased by 153%. This property highlights the advantage of our approach compared to the observer design in [11]. Note that for other values of the decay rate we still have improvements, but the numbers are very large so they will not be reached in practice.

Next we consider the compact set of the state $x_1 \in [-\pi,\ \pi]$ and $\sigma = 65[rad/s]$. We focus only on the performances of the observer, so we consider the unforced-case, where we have no input signal. The initial condition for the system is $x_0 = [-0.1,\ 0.7]^T$.

In what follows, we test the performances of three observers. The first one is the observer designed using the approach presented in [11], with $\omega = 0.4$, because this is the smallest value for which feasible solution have been found with respect to the given $\sigma = 65[rad/s]$. Next we set $\omega = 0.31$, and the second observer is based on Theorem 1 with no injection term ($L_\psi = 0$), while the third observer is with the injection term.

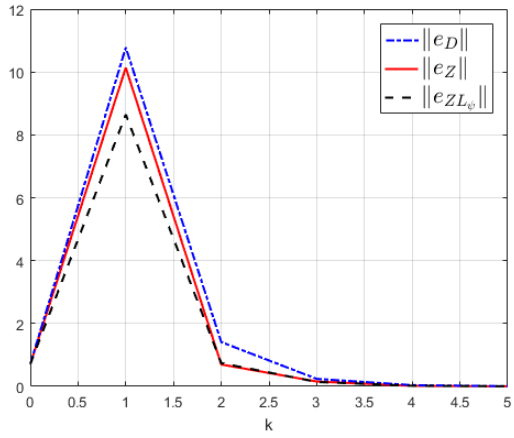

Fig. 3. Norm of the errors

The norm of the estimation errors can be seen on Fig. 3, where the sample index is on the horizontal axis, $\|e_D\|$ is the norm of the error with Theorem 1 in [11], $\|e_Z\|$ is with Theorem 1, when $L_\psi = 0$, and $\|e_{ZL_\psi}\|$ is with the injection term. For all three cases the initial conditions for the observers are $\hat{x}_0 = [0,\ 0]^T$. It can be seen that the convergence is faster in our case, and also the maximum error is reduced, especially when we have the injection term.

As it was already mentioned in Section IV, for controller design we have the advantage that we do not need the sector-bound condition. For the inverted pendulum model in (80) the nonlinear consequent is $\psi(x(k)) = x_2(k)^2 + \sigma x_2(k)$, with the assumption that $|x_2| \leq \sigma$. The sector-bound condition for $\psi(\cdot)$ is $\psi(x(k)) \in \text{co}\{0,\ Ex(k)\}$, where $E = [0,\ 2\sigma]$, so the sector bound depends on the double of the maximum angular velocity. Similarly to observer design, here also greater values of σ are better.

In (10) we use the form $B_z G_z \psi(Hx)$, while in [11] only $\tilde{G}_z \psi(x)$ is used. For the comparison, we have:

$$\begin{aligned} \tilde{G}_1 =& \tilde{G}_3 = \tilde{G}_5 = \tilde{G}_7 = \begin{bmatrix} 0 \\ -0.45e-3 \end{bmatrix}, \\ \tilde{G}_2 =& \tilde{G}_4 = \tilde{G}_6 = \tilde{G}_8 = \begin{bmatrix} 0 \\ 0.45e-3 \end{bmatrix}. \end{aligned} \tag{82}$$

To highlight the advantage of our approach we consider a decay rate $\omega_c = 0.64$, to have a fast convergence to the stabilization point. Using this decay rate our LMI conditions provide feasible solutions for any value of σ, while Corollary 1 in [11] provides feasible solutions only for $\sigma \leq 42[rad/s]$. This proves that under these conditions our LMIs are less restrictive than the ones in Corolloary 1 in [11]. Note that for greater values of the decay rate we still have improvements, but the numbers are very large so they will not be reached in practice.

As it was mentioned in Section IV for observer-based controller design we need both observer and controller design conditions. For example, we consider Theorem 1 and Corollary 1 in [11]. We would like to have a decay-rate $\omega_o = 0.31$ for observer design, which leads to a maximum angular velocity $\sigma = 45[rad/s]$ and for controller design we consider a decay-rate $\omega_c = 0.64$, which leads to $\sigma = 42[rad/s]$. So in the case of observer-based controller design the approaches of [11] provides theoretical guarantees only for $\sigma = 42[rad/s]$, due to the limitation of the controller.

On the other hand, using our observer-based controller design approach in Theorem 2 we do not have the sector-bound restriction for controller design and the observer design conditions are less restrictive, therefore we have theoretical guarantee for $\sigma = 114[rad/s]$.

B. Simulation results

The compact set of the state-space on which the TS model is constructed is given by: $x_1 \in [-\frac{\pi}{3}, \frac{\pi}{3}]$ and $x_2 \in [-\sigma, \sigma]$, with $\sigma = 15[rad/s]$. Since we have 3 nonlinearities, $\rho_1(x_1)$, $\rho_2(x_1)$, and $\rho_3(x_1)$, all depending on measured variable x_1, we obtain an $s2^3 = 8$ rule TS fuzzy model, with local matrices:

$$\begin{aligned} A_1 =& A_2 = A_3 = A_4 = \begin{bmatrix} 1 & 0.01 \\ 0 & 0.85 \end{bmatrix}, \\ A_5 =& A_6 = A_7 = A_8 = \begin{bmatrix} 1 & 0.01 \\ 0 & 1.05 \end{bmatrix}, \\ B_1 =& B_2 = B_5 = B_6 = \begin{bmatrix} 0 \\ -0.0473 \end{bmatrix}, \\ B_3 =& B_4 = B_7 = B_8 = \begin{bmatrix} 0 \\ -0.0221 \end{bmatrix}, \\ G_1 =& G_3 = G_5 = G_7 = -0.0176, \\ G_2 =& G_4 = G_6 = G_8 = 0.0176. \end{aligned} \tag{83}$$

We apply Theorem 1 for the observer design. At the first try we obtained $L_{\psi i}$ terms that were close to each other, therefore we consider a constant L_ψ. The following observer gains were obtained:

$$\begin{aligned} L_\psi =& -11.0232,\ L_1 = \begin{bmatrix} 1.11 \\ 9.89 \end{bmatrix},\ L_2 = \begin{bmatrix} 1.11 \\ 9.83 \end{bmatrix}, \\ L_3 =& \begin{bmatrix} 1.11 \\ 9.87 \end{bmatrix},\ L_4 = \begin{bmatrix} 1.11 \\ 9.82 \end{bmatrix},\ L_5 = \begin{bmatrix} 1.12 \\ 13.55 \end{bmatrix}, \\ L_6 =& \begin{bmatrix} 1.10 \\ 12.75 \end{bmatrix},\ L_7 = \begin{bmatrix} 1.12 \\ 12.95 \end{bmatrix},\ L_8 = \begin{bmatrix} 1.10 \\ 12.75 \end{bmatrix}. \end{aligned} \tag{84}$$

Next, we apply Lemma 4 for controller design. To reduce the computational complexity of the LMIs, Q is defined constant, and the obtained controller gains are:

$$\begin{aligned} K_1 =& \begin{bmatrix} -0.65 & 0.05 \end{bmatrix},\ K_2 = \begin{bmatrix} -0.65 & 0.05 \end{bmatrix}, \\ K_3 =& \begin{bmatrix} -0.70 & 0.14 \end{bmatrix},\ K_4 = \begin{bmatrix} -0.70 & 0.14 \end{bmatrix}, \\ K_5 =& \begin{bmatrix} 0.24 & -0.55 \end{bmatrix},\ K_6 = \begin{bmatrix} 0.24 & -0.55 \end{bmatrix}, \\ K_7 =& \begin{bmatrix} 0.30 & -0.59 \end{bmatrix},\ K_8 = \begin{bmatrix} 0.30 & -0.59 \end{bmatrix}, \\ Q^{-1} =& \begin{bmatrix} 4.29 & 3.03 \\ 3.04 & 6.81 \end{bmatrix}. \end{aligned} \tag{85}$$

The initial condition for the simulation is $x(0) = [\frac{\pi}{6}, 0.4]^T$, and for the observer $\hat{x}(0) = [\frac{\pi}{6}, 0]^T$. The system states can be seen in Fig. 4. The obtained results show that the system states are stabilized at the unstable equilibrium point and the estimated states converge to the true states (Fig. 5).

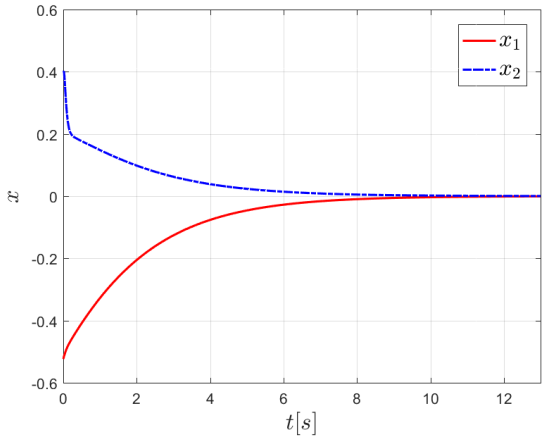

Fig. 4. Closed-loop system states with initial condition $x(0) = [\frac{\pi}{6}, 0.4]^T$ -simulation

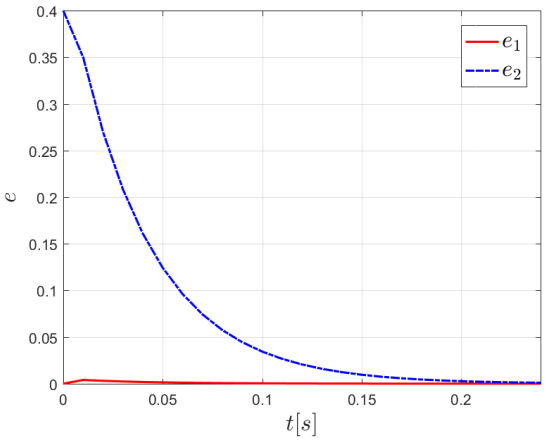

Fig. 5. Estimation error

C. Experimental results

For the real application the control input is bounded, $u \in [-1, 1]$, so the generated input signal is not enough to move the pendulum in the pointing up position. To overcome this issue a destabilizing control law is used which is applied when $|x_1| > 0.3\,[\text{rad}]$. For destabilization, we use the system's inertia: for example, if the angle is negative, we move the cart in the opposite direction with maximum input for $5[s]$, then suddenly a brake is applied, so the rod of the pendulum is moving from the negative angle towards 0. When the angle is $|x_1| < 0.3\,[\text{rad}]$, then the observer-based control law is applied.

The angle of the physical model is limited to move on the range $x_1 \in [-\frac{\pi}{6}, \frac{\pi}{6}]$, see Fig. 6.

The obtained output is denoted with y_Z and is shown in Fig. 7. As it can be seen the controller is stabilizing faster than in simulation due to the inertia of the pendulum, which gives the system a large angular velocity.

To provide another perspective from the experimental point of view, we compare our experiments to the approach presented in [31]. To apply the approach in [31] we approximate (78) as

$$\dot{x} = A_z x + B_z u,$$

Fig. 6. Pendulum on a cart

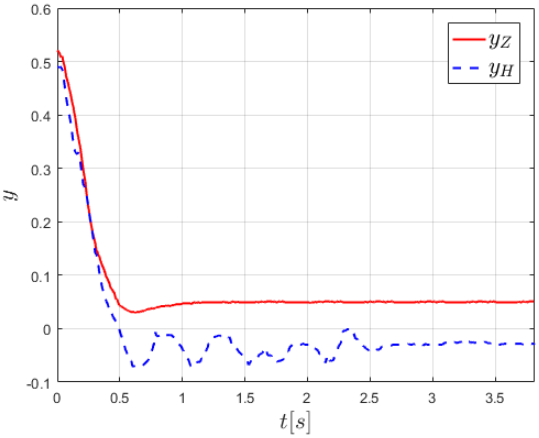

Fig. 7. Real system output, y_Z- our approach, y_H approach from [31]

with matrices:

$$A_1 = \begin{bmatrix} 0 & 1 \\ \frac{mgl}{\mu} & -\frac{\gamma}{\mu} \end{bmatrix},\ B_1 = \begin{bmatrix} 0 \\ -\frac{aml}{\mu} \end{bmatrix},$$
$$A_2 = \begin{bmatrix} 0 & 1 \\ \frac{mgl}{\mu_\kappa} & -\frac{\gamma}{\mu_\kappa} \end{bmatrix}, B_2 = \begin{bmatrix} 0 \\ -\frac{aml\kappa}{\mu_\kappa} \end{bmatrix}, \quad (86)$$

where $\kappa = \cos\left(\frac{\pi}{6}\right)$, $\mu = J + ml^2 - am^2l^2$, and $\mu_\kappa = (J+ml^2) - am^2l^2\cos\left(\frac{\pi}{6}\right)^2$. The membership functions are the same as in [31], therefore they are not presented here. Applying Lemma 1 in [31], the controller gains are:

$$K_1 = \begin{bmatrix} -30.76 & -4.38 \end{bmatrix},\ K_2 = \begin{bmatrix} -30.73 & -4.73 \end{bmatrix}. \quad (87)$$

Since the angular velocity is not measured we use the approximation $x_2 = \frac{x_1(k) - x_1(k-1)}{T_s}$. The experimental results obtained with this controller are given in Fig. 7 (y_H).

In both cases the angle is not exactly 0 in steady state. These small deviations are there because of the friction of the electro-mechanical elements. To make the motor move, the input signal should pass a certain threshold to overcome the friction force of the motor, but since we are very close to the pointing up position, the generated torque is not enough to pass this threshold. Furthermore, we have a relatively high static friction due to the other mechanical parts of the system, which further increases the threshold.

The approach we propose provides a smoother result, but a somewhat larger steady-state error. The controller of [31]

provides a smaller steady-state error, but with a larger settling time due to the oscillations around the stabilization point.

VI. Conclusions and Future work

This paper presented a novel observer-based control design approach for nonlinear systems with local nonlinearities. Two types of nonlinearities were considered: measured and unmeasured state nonlinearities. The nonlinearities that depend on measured states were handled using TS fuzzy modelling, while those that depend on unmeasured states were kept as local nonlinearities. The new approach of observer and controller design proved to be less conservative than existing results in the literature. We showed that the control and the observer can be independently designed. Finally, the design was illustrated on a pendulum on a cart example.

In the future we will consider model uncertainties in the design. We will also apply our method for more complex real systems.

References

[1] H. K. Khalil, *Nonlinear Systems, Third edition*. Prentice Hall, Upper Saddle River, NJ 07458, 2000.

[2] H. Ohtake, K. Tanaka, and H. Wang, "Fuzzy modeling via sector nonlinearity concept," in *Proceedings of the Joint 9th IFSA World Congress and 20th NAFIPS International Conference*, vol. 1, Vancouver, Canada, July 2001, pp. 127–132.

[3] J. Dong and G.-H. Yang, "Robust static output feedback control synthesis for linear continuous systems with polytopic uncertainties," *Automatica*, vol. 49, no. 6, pp. 1821–1829, 2013.

[4] ——, "Reliable state feedback control of T–S fuzzy systems with sensor faults," *IEEE Transactions on Fuzzy Systems*, vol. 23, no. 2, pp. 421–433, 2014.

[5] Zs. Lendek, R. Babuška, and B. D. Schutter, "Stability of cascaded fuzzy systems and observers," *IEEE Transactions on Fuzzy Systems*, vol. 17, no. 3, pp. 641–653, 2009.

[6] Zs. Lendek, T. M. Guerra, and B. De Schutter, *Stability analysis and nonlinear observer design using Takagi-Sugeno fuzzy models*. Springer, 2011.

[7] V. Estrada-Manzo, Zs. Lendek, T. M. Guerra, and P. Pudlo, "Controller design for discrete-time descriptor models: a systematic LMI approach," *IEEE Transactions on Fuzzy Systems*, vol. 23, no. 5, pp. 1608–1621, 2014.

[8] R. Subramaniam, D. Song, and Y. H. Joo, "TS Fuzzy-based Sliding Mode Control Design for Discrete-time Nonlinear Model and its Applications," *Information Sciences*, 2020.

[9] R. Subramaniam and Y. H. Joo, "Passivity-based fuzzy ISMC for wind energy conversion systems with PMSG," *IEEE Transactions on Systems, Man, and Cybernetics: Systems*, 2019.

[10] G. Nagamani and S. Ramasamy, "Dissipativity and passivity analysis for discrete-time T–S fuzzy stochastic neural networks with leakage time-varying delays based on Abel lemma approach," *Journal of the Franklin Institute*, vol. 353, no. 14, pp. 3313–3342, 2016.

[11] J. Dong, Y. Wang, and G.-H. Yang, "Output feedback fuzzy controller design with local nonlinear feedback laws for discrete-time nonlinear systems," *IEEE Transactions on Systems, Man, and Cybernetics, Part B (Cybernetics)*, vol. 40, no. 6, pp. 1447–1459, 2010.

[12] M. Benallouch, M. Boutayeb, and H. Trinh, "H_∞ Observer-Based Control for Discrete-Time One-Sided Lipschitz Systems with Unknown Inputs," *SIAM Journal on Control and Optimization*, vol. 52, no. 6, pp. 3751–3775, 2014.

[13] S. Ibrir, "Circle-criterion approach to discrete-time nonlinear observer design," *Automatica*, vol. 43, no. 8, pp. 1432–1441, 2007.

[14] J. Grizzle and P. Kokotovic, "Feedback linearization of sampled-data systems," *IEEE Transactions on Automatic Control*, vol. 33, no. 9, pp. 857–859, 1988.

[15] J. Dong and G.-H. Yang, "Observer-based output feedback control for discrete-time TS fuzzy systems with partly immeasurable premise variables," *IEEE Transactions on Systems, Man, and Cybernetics: Systems*, vol. 47, no. 1, pp. 98–110, 2016.

[16] M. Arcak and P. Kokotović, "Nonlinear observers: A circle criterion design," *Conference on Decision and Control, Phoenix, AZ, USA, pp. 4872-4876*, 1999.

[17] ——, "Observer-based control of systems with slope-restricted nonlinearities," *Transaction on Automatic Control, 46, pp. 1146-1150*, 2001.

[18] A. Zemouche, M. Boutayeb, and G. I. Bara, "Observers for a class of Lipschitz systems with extension to H_∞ performance analysis," *Systems & Control Letters*, vol. 57, no. 1, pp. 18–27, 2008.

[19] M. Chong, R. Postoyan, D. Nesic, L. Kuhlmann, and A. Varsavsky, "A robust circle criterion observer with application to neural mass models," *Automatica, Elsevier, 48 (11), pp.2986-2989*, 2012.

[20] A. Zemouche, R. Rajamani, B. Boulkroune, H. Rafaralahy, and M. Zasadzinski, "H_∞ circle criterion observer design for Lipschitz nonlinear systems with enhanced LMI conditions," in *2016 American Control Conference (ACC)*. IEEE, 2016, pp. 131–136.

[21] K. Chaib Draa, A. Zemouche, M. Alma, H. Voos, and M. Darouach, "A discrete-time nonlinear state observer for the anaerobic digestion process," *International Journal of Robust and Nonlinear Control*, vol. 29, no. 5, pp. 1279–1301, 2019.

[22] Z. Nagy and Zs. Lendek, "Observer-based controller design for Takagi-Sugeno fuzzy systems with local nonlinearities," *International Conference on Fuzzy Systems FuzzIEEE, New Orleans, LA, USA*, 2019.

[23] J. Dong, Y. Wang, and G.-H. Yang, "Control synthesis of continuous-time T-S fuzzy systems with local nonlinear models," *IEEE Transactions on Systems, Man, and Cybernetics—part B: Cybernetics, 39 (5), pp. 1245-1258*, 2009.

[24] H. Moodi and M. Farrokhi, "Robust observer design for Sugeno systems with incremental quadratic nonlinearity in the consequent," *International Journal of Applied Mathematics and Computer Science, 23, pp. 711-723*, 2013.

[25] ——, "Robust observer-based controller design for Takagi Sugeno systems with nonlinear consequent parts," *Fuzzy Sets and Systems, 273, pp. 141-154*, 2015.

[26] A.-T. Nguyen, P. Coutinho, T.-M. Guerra, and R. Palhares, "Control synthesis for fuzzy systems with local nonlinear models subject to actuator saturation," in *2019 IEEE International Conference on Fuzzy Systems (FUZZ-IEEE)*. IEEE, 2019, pp. 1–6.

[27] S. Boyd, L. El Ghaoui, E. Féron, and V. Balakrishnan, *Linear Matrix Inequalities in System and Control Theory*, ser. Studies in Applied Mathematics. Philadelphia, PA, USA: Society for Industrial and Applied Mathematics, 1994.

[28] H. Tuan, P. Apkarian, T. Narikiyo, and Y. Yamamoto, "Parameterized linear matrix inequality techniques in fuzzy control system design," *IEEE Transactions on Fuzzy Systems*, vol. 9, no. 2, pp. 324–332, 2001.

[29] K. C. Draa, H. Voos, M. Alma, A. Zemouche, and M. Darouach, "LMI-based trajectory tracking for a class of nonlinear systems with application to an anaerobic digestion process," *Annual American Control Conference, Wisconsin Center, Milwaukee, USA, pp. 4393-4397*, 2018.

[30] M. Bernal and P. Husek, "Non-quadratic performance design for Takagi-Sugeno fuzzy systems," *International Journal of Applied Mathematics and Computer Science*, vol. 15, no. 3, pp. 383–391, 2005.

[31] J. Huang, M. Ri, D. Wu, and S. Ri, "Interval type-2 fuzzy logic modeling and control of a mobile two-wheeled inverted pendulum," *IEEE Transactions on Fuzzy Systems*, vol. 26, no. 4, pp. 2030–2038, 2017.